

Novel stochastic approach for Gutzwiller matrix elements: Two-dimensional Hubbard model

P. G. McQueen and C. S. Wang

Center for Superconductivity Research, Department of Physics, University of Maryland, College Park, Maryland 20742-4111

(Received 18 November 1988; revised manuscript received 6 March 1989)

A new approach is presented for variational Monte Carlo simulations of Hubbard-Anderson models using Gutzwiller projection operators to restrict charge fluctuations in noninteracting wave functions. The Gutzwiller matrix elements are mapped onto a statistical model, which is evaluated using a stochastic algorithm that is normally applied to finite-temperature simulation. The method has been successfully tested for one-dimensional (1D) Hubbard and 1D Anderson models, and results are presented for the 2D Hubbard model. We find a region close to the half-filled limit where the Gutzwiller states of different magnetic ordering are very close in energy.

There has been a great deal of interest recently in the properties of systems in which the electrons are almost localized. This is evident from the heavy-fermion superconductors and the high-temperature superconductors where many unconventional pairing mechanisms of electronic origin have been proposed. These systems are characterized by a strong Hubbard-type Coulomb repulsion, $H_1 = U \sum_i n_{i\uparrow} n_{i\downarrow}$, which suppresses double occupation on a given site, but the systems are better described as Fermi liquids than as localized electrons.

Gutzwiller¹ proposed to solve such a problem using a variational wave function $|\Psi_g\rangle$ in which a projection operator P_g is applied to restrict the charge fluctuations in a noninteracting wave function $|\Psi_0\rangle$:

$$|\Psi_g\rangle = P_g |\Psi_0\rangle = \prod_{i=1}^V [1 - (1-g)n_{i\uparrow}n_{i\downarrow}] |\Psi_0\rangle, \quad (1)$$

where g is the variational parameter, n_{is} is the occupation number operator for site i and spin s , and V is the number of sites. Most methods evaluate the Gutzwiller matrix elements by expressing $|\Psi_g\rangle$ as a Jastrow wave function and then evaluate the Slater determinants stochastically.²⁻⁵ Recently, Metzner and Vollhardt have introduced a new analytical procedure to calculate 1D Hubbard model.⁶ In this paper, we introduce an alternative approach that maps the expectation values in the Gutzwiller ground state onto a statistical-mechanical model which can be evaluated in a similar way to finite-temperature Monte Carlo simulations, but with significant saving in computational efforts. We have successfully tested this procedure for the one-dimensional (1D) Hubbard and Anderson models. Among our major results for the 2D Hubbard model presented here, we find (1) long-range antiferromagnetic order exists in the half-filled limit ($\nu=1$ electron per site), (2) the Gutzwiller states of different magnetic order can be very close in energy ($\nu=0.9375$), and (3) the ground state is paramagnetic further away from the half-filled limit ($\nu=0.8$). The corresponding momentum densities exhibit the characteristics of an insulator, an almost localized Fermi liquid, and a normal metal, respectively. Results will be compared with previous calculations.⁷⁻⁹

The Gutzwiller matrix elements can be written as

$$\langle A \rangle = \langle \Psi_0 | P_g A P_g | \Psi_0 \rangle / \langle \Psi_0 | P_g^2 | \Psi_0 \rangle \\ = \lim_{\beta \rightarrow \infty} Z_g^{-1} \text{tr}[\exp(-\beta \mathcal{H}) P_g A P_g], \quad (2)$$

where $Z_g = \text{tr}[\exp(-\beta \mathcal{H}) P_g^2]$ is a pseudopartition function, and $|\Psi_0\rangle$ is the ground state of a noninteracting Hamiltonian \mathcal{H} . The Hubbard-Stratonovich transformation is used to rewrite P_g^2 in the form of an S matrix in quantum-field theory:

$$P_g^2 = \prod_{i=1}^V [1 - (1-g^2)n_{i\uparrow}n_{i\downarrow}] = \left(\frac{1}{2}\right)^V \sum_{\{\sigma\}} \exp(h_{\{\sigma\}}), \quad (3)$$

For a given Ising-spin configuration of the lattice $\{\sigma_i = \pm 1\}$,

$$h_{\{\sigma\}} = \sum_i \alpha \sigma_i (n_{i\uparrow} - n_{i\downarrow}) + K (n_{i\uparrow} + n_{i\downarrow}) \quad (4)$$

with $K = \ln(g)$ and $\cosh(\alpha) = 1/g$. The partition function becomes

$$Z_g = \left(\frac{1}{2}\right)^V \sum_{\{\sigma\}} \text{tr} \exp(h_{\{\sigma\}}/2) \exp(-\beta \mathcal{H}) \exp(h_{\{\sigma\}}/2) \\ = \left(\frac{1}{2}\right)^V \sum_{\{\sigma\}} \text{tr} \prod_s \text{tr}[\exp(\gamma_{\{\sigma\}}^s)]. \quad (5)$$

Since \mathcal{H} , $h_{\{\sigma\}}$, and $[\mathcal{H}, h_{\{\sigma\}}]$ are single-particle operators, $\gamma_{\{\sigma\}}^s = \sum_{i,j} \gamma_{ij}^s c_{is}^\dagger c_{js}$ is also a single-particle operator. Performing the trace gives

$$Z_g = \left(\frac{1}{2}\right)^V \sum_{\{\sigma\}} \prod_s \det(I + \exp \Gamma_{\{\sigma\}}^s), \quad (6)$$

where $\Gamma_{\{\sigma\}}^s$ is a $V \times V$ matrix $[\gamma_{ij}^s]$ for $s = \uparrow, \downarrow$. The Metropolis algorithm is used to sum over the Ising-spin configuration for the lattice. We follow the procedure of Blankenbecler, Scalapino, and Sugar¹⁰ to calculate the determinant ratio and updates $(I + \exp \Gamma_{\{\sigma\}}^s)^{-1}$, if a change in the Ising configuration is made by one spin flip. The computational effort for one spin flip grows as V^2 so that one sweep through the lattice takes $\approx V^3$ steps. This algorithm has been used for Monte Carlo simulation of the exact partition functions of correlated fermionic sys-

tems at temperature T .^{7,10}

$$\begin{aligned} Z &= \text{tr} e^{-(H_0 - \mu N + H_1)/kT} \\ &\approx \text{tr} \prod_{l=1}^L e^{-\Delta\tau(H_0 - \mu N)} e^{-\Delta\tau H_1} \end{aligned} \quad (7)$$

where μ is the chemical potential, and $N = \sum_{i,s} n_{is}$. For the nearest-neighbor one-band Hubbard model, $H_0 = t \sum_{\langle i,j \rangle} \sum_s c_{is}^\dagger c_{js}$. Note that an imaginary Matsubara time index $\Delta\tau = 1/(kTL)$ is introduced for the Trotter breakup in Eq. (7), which raises the computational efforts to V^3/T . Furthermore, the errors introduced by the Trotter breakup increase with decreasing T and increasing U . Since H_1 does not appear in the pseudo partition function Z_g , there is no Trotter breakup of Z_g , and no Matsubara time index in our approach. Thus, the computational efforts and the numerical accuracy are significantly improved. On the other hand, variation calculations depend on the variational freedom in $|\Psi_g\rangle$. The close resemblance of our approach to exact simulations at higher temperature provides a cross reference for the ground state properties and finite size scaling with little additional efforts.

The Green's function for spin s and a given Ising configuration $[\sigma]$, can be written as

$$\begin{aligned} G_{[\sigma],ij}^s &= \text{tr} [\exp(\gamma_{[\sigma]}^s) c_{is} c_{js}^\dagger] \\ &= [I + \exp \Gamma_{[\sigma]}^s]_{ij}^{-1}. \end{aligned} \quad (8)$$

If $[A, P_g] = 0$, as for the number per site, or for spin-spin or density-density correlations, then

$$\langle A \rangle = \left(\frac{1}{2}\right)^V Z_g^{-1} \text{tr} \prod_{[\sigma]} [\exp(\gamma_{[\sigma]}^s) A]. \quad (9)$$

If A is a two- or three-particle correlation, the Wick's theorem can be used for each Ising configuration $[\sigma]$ to decompose A into products of G_{ij} . If $[A, P_g] \neq 0$, it can be shown that if $i \neq j$,

$$\begin{aligned} P_g c_{is} c_{js}^\dagger P_g &= \left(\frac{1}{2}\right)^V [g \cosh^2(a/2)]^{-1} \\ &\quad \times \sum_{[\sigma]} \exp(h_{[\sigma]}/2) c_{is} c_{js}^\dagger \exp(h_{[\sigma]}/2). \end{aligned}$$

Then,

$$\langle c_{is} c_{js}^\dagger \rangle = [g \cosh^2(a/2)]^{-1} \sum_{[\sigma]} [I + \exp(\Gamma_{[\sigma]}^s)]_{i,j}^{-1}. \quad (10)$$

For 1D Hubbard model, our results are in good agreement with the variational Monte Carlo simulations of Gros, Joynt, and Rice,⁵ who have refined the weighting of the Slater coefficients in the $g=0$ limit to study the chains up to $\approx 10^4$ sites. Our approach for a 1D Hubbard ring of 100 sites takes approximately 10 CPU min on CRAY 1-XMP. However, the efficiency of this algorithm is the same in any dimension, and the procedure can be easily generalized to one-particle operators that do not commute with P_g . We have also applied the new algorithm to the 1D Anderson model and found excellent agreement with the variational Monte Carlo simulations of Shiba.⁸ In the case of Hubbard models, we used $\beta \approx 30$, with approximately 2000 lattice sweeps to warm up the Ising spins, and 1000 to 2000 additional sweeps separated by 4 sweeps

for the Green's-function measurements, while in the case of the Anderson model, where there is an enormous density of states near the Fermi level, we used $\beta \approx 30000$, and 10000 or more warm-up sweeps. Our results for the 2D Anderson lattices will be presented elsewhere; here, we discuss the results of the 2D Hubbard model.

For the Hubbard model, $|\Psi_0\rangle$ can be nonmagnetic (NM), antiferromagnetic (AFM), or ferromagnetic (FM). We vary g , and in the case of AFM or FM states the built-in moment, to minimize the ground-state energy. In the half-filled limit ($\nu=1$ electron per site), our scaling analysis shows long-range antiferromagnetic order due to Fermi-surface nesting, which is in close agreement with earlier calculations. In a recent variational Monte Carlo simulation, Shiba and Yokoyama⁴ found the long-range antiferromagnetic order persists to $\nu \geq 0.9$ (depending on U). By contrast, finite-temperature Monte Carlo simulations of Hirsch⁷ indicate that the long-range order is always destroyed for non-half-filled cases. The conclusions of Hirsch are based on finite-size scaling analysis of lattices up to $V=8 \times 8$ in spatial size, at temperature $\beta=0.75\sqrt{V}$. These results may be consistent with a more recent calculation of Sorella *et al.*⁹ who solved the Langevin dynamics for a 16×16 lattice at $\beta=24$ and $U=4$, although they are uncertain if the spin-correlation functions decay exponentially or as a power law. In fact, they found that the corresponding spin-spin correlations for the $U=0$ Fermi liquid look quite similar. Comparing the energies of the AFM and NM states, our variational calculations agree with the phase diagram of Shiba and Yokoyama. We found that the Gutzwiller states of different magnetic ordering can be very close in energy for $\nu=0.9735$, which may explain the discrepancy between finite temperature and variational simulations.

Figure 1 shows the finite-size variation of the kinetic energy and the Coulomb energy per site for $U=4$ and $t=1$. These energies are extrapolated linearly in $1/V$ to yield the ground-state energy. In the half-filled limit ($\nu=1.0$), the AFM ground-state energy (-0.842) is significantly lower than the NM state (-0.780) (with an uncertainty of ± 0.007), while for the $\nu=0.9375$ case, the AFM energies (-0.913) is much closer to the NM state (0.898). Thus the loss of long-range order in finite-temperature simulations may reflect thermal fluctuations between nearly degenerate states. Otherwise, the discrepancy is an indication of the limitation of our variational states to describe the short-range spin fluctuations. In particular, Anderson¹¹ has proposed that the ground state of the Hubbard model may be a resonating-valence-bond (RVB) phase consisting of highly degenerate, singlet pairs of electrons, superconductivity can then be induced by doping away from the half-filled limit. For moderate doping, the results of Sorella *et al.*⁹ seem to suggest an unusual phase that resembles RVB fluctuations, while earlier work of Hirsch⁷ seems to indicate an ordinary paramagnetic metallic phase. Recent variational Monte Carlo simulations for 2D Heisenberg models indicate that antiferromagnetism is destroyed by doping and the paramagnetic RVB states becomes stable.¹²

Figure 2 shows our finite-size-scaling analysis of the Fourier transform of the spin-spin correlation $S(\pi, \pi)$ for

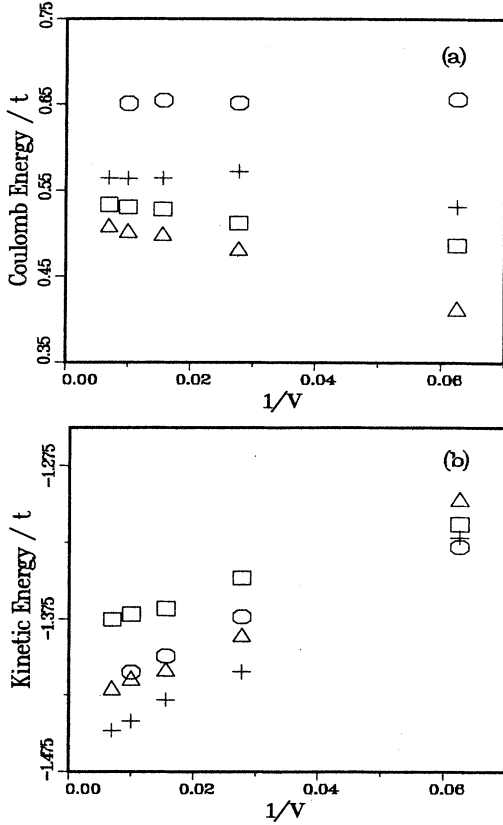


FIG. 1. Finite-size scaling analysis of (a) the kinetic energy per site, and (b) the Coulomb energy per site vs $1/V$, where V is the number of sites and $U=4$. Results are presented for $\nu=1.000$ with AFM states (\square); NM states (\circ), $\nu=0.9375$ for AFM state (\triangle), and NM state ($+$).

$U=16$, with $\nu=1.000$, 0.9375 , and 0.800 . We used the Gutzwiller ground-states wave functions, which are AFM for the first two cases, and NM for $\nu=0.800$. In the thermodynamic limit ($V \rightarrow \infty$), $S(\pi, \pi)$ remains finite for the AFM states and vanishes for the NM states. If the nearly

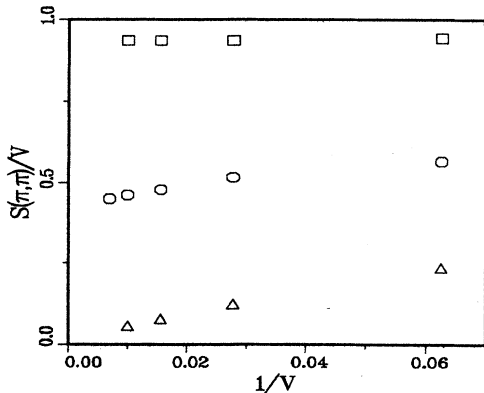


FIG. 2. Finite-size-scaling analysis of the Fourier transform of the spin-spin correlations $S(\pi, \pi)/V$ for $U=16$, with $\nu=1.000$ (\square), 0.9375 (\circ), and 0.800 (\triangle).

degenerate NM state were used for $\nu=0.9375$, $S(\pi, \pi)$ would also vanish. These results are similar to the phase diagram predicted by Shiba and Yokoyama,⁴ although there are quantitative differences between the two calculations for smaller lattices because they use boundary conditions that are periodic in one direction and antiperiodic in the other, while our boundary conditions are periodic in both directions. They also predicted a FM region very near the half-filled case for $U \cong 50t$.

The momentum density of the AFM state for $U=4$, $\nu=0.9375$, is shown in Fig. 3. Note that this density is remarkably similar to the results of Sorella *et al.*⁹ for $U=4$, $\nu=226/256$. They concluded from the slope at the Fermi momentum (k_F) that it may be an unusual insulating RVB phase. We have not considered here the RVB state in our variational calculations. The momentum density in Fig. 3 seems to suggest that the AFM state has a well-defined Fermi surface. For a finite-size cluster, it is difficult to determine precisely the slope at k_F , but a metallic phase is the ground state of the mean-filled approximation, and quantum fluctuations which broaden the spectral functions should not reverse this conclusion. Antiferromagnetism is stabilized by a lowering of the electronic energy due to a magnetic contribution arising from Fermi-surface nesting. In the half-filled limit, the system becomes an insulator because band gaps are opened at k_F . Away from the half-filled limit, however, k_F is incommensurate with the antiferromagnetic order, so that the system is a metal. The incommensuratness is a unique feature of finite-size simulations, which may be modified in the thermodynamic limit.

Our results for $U=16$ with (a) $\nu=1.000$, (b) $\nu=0.9375$, and (c) $\nu=0.800$, respectively, are shown in Fig. 4. In the half-filled limit, it is an antiferromagnetic insulator so that there is no Fermi-surface effect. It gradually loses long-range antiferromagnetic order as the filling factor is reduced. As can be seen from Figs. 4(b) (AFM) and 4(c) (NM), the volume enclosed by the Fermi surface appears to be reproduced correctly in accordance with Luttinger's theory,¹³ while some of the spectral weight is shifted to higher momentum due to electron correlation. It is interesting to note in Fig. 4(c), that there is a depletion of $n(k)$ for $k > k_F$ near the Fermi surface. The extra depletion leads to a jump at the Fermi

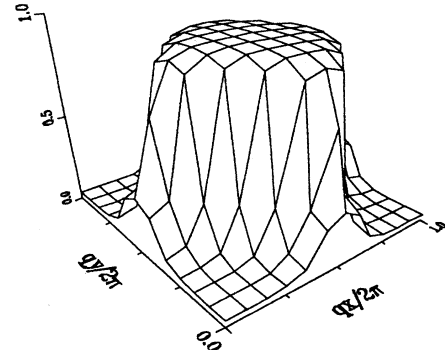


FIG. 3. Momentum density for $U=4$, $\nu=0.9375$.

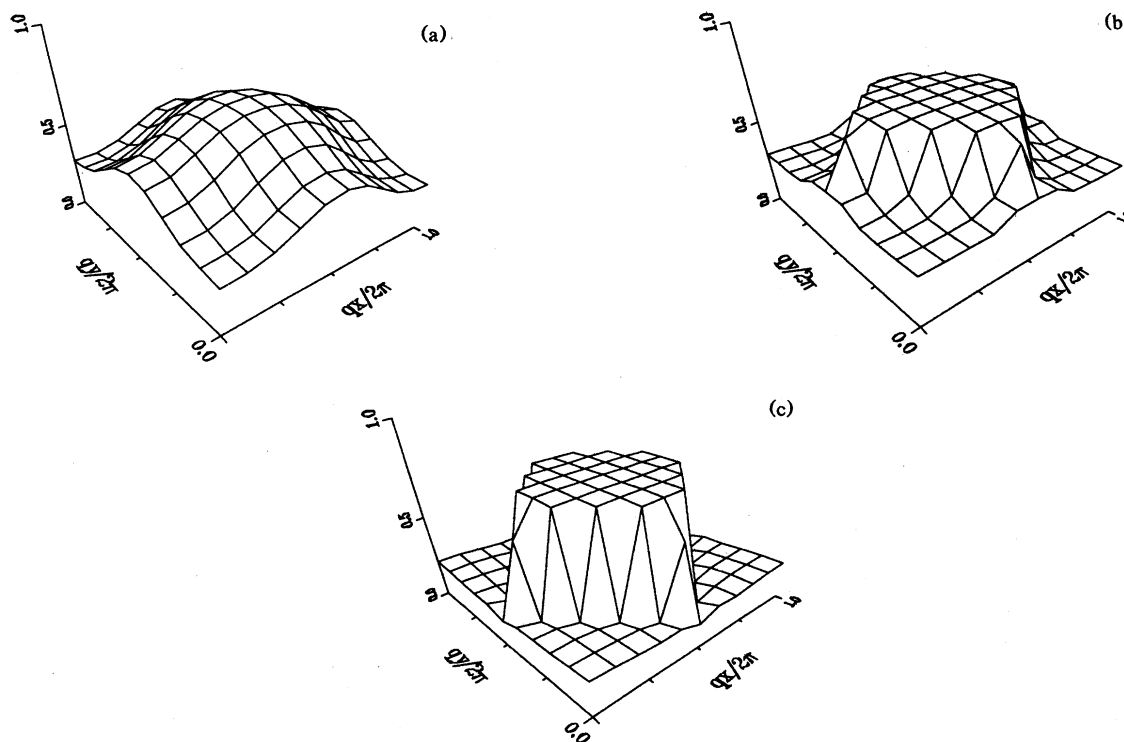


FIG. 4. Momentum density for $U=16$ with (a) $\nu=1.000$, (b) $\nu=0.9375$, and (c) $\nu=0.800$.

surface which is the renormalization factor. In the case of 1D Hubbard chains, an extra depletion has also been observed in the variational Monte Carlo simulations of Gros, Joynt, and Rice⁵ but is absent when the Gutzwiller approximation formula, which is a mean-field approximation for the Gutzwiller matrix element, is used. By contrast, a sharp drop at k_F appears in the Hartree-Fock AFM state for 2D Hubbard model with $U=4$ and $\nu=226/256$,⁹ but not in the corresponding Gutzwiller ground state shown in Fig. 3 or the simulations of Sorella *et al.*⁹ Thus, the renormalization factor is a very sensitive test, and our varia-

tional calculations are in good agreement with the simulations of Sorella *et al.*⁹

We thank T. Einstein and P. A. Sterne for comments on the manuscript, and M. P. Gelfand and N. C. Bartelt for a critique of the finite-size scaling. This work was supported in part by the National Science Foundation Grant No. DMR-86-01708. Computations were carried out under the auspices of the National Science Foundation at the Pittsburgh Supercomputer Center and at the University of Maryland.

¹For a review of the historical development of the Gutzwiller state, see D. Vollhardt, *Rev. of Mod. Phys.* **56**, 99 (1984).

²P. Horsch and T. A. Kaplan, *J. Phys. C* **16**, L1203 (1983).

³H. Yokoyama and H. Shiba, *J. Phys. Soc. Jpn.* **56**, 1490 (1987); H. Shiba and H. Yokoyama, *ibid.* **56**, 3582 (1987).

⁴H. Shiba and H. Yokoyama, *Physica B* **148**, 264 (1987).

⁵C. Gros, R. Joynt, and T. M. Rice, *Phys. Rev. B* **36**, 381 (1987).

⁶W. Metzner and D. Vollhardt, *Phys. Rev. Lett.* **59**, 121 (1987); F. Gebhard and D. Vollhardt, *ibid.* **59**, 1472 (1987).

⁷J. E. Hirsch, *Phys. Rev. B* **31**, 4403 (1985).

⁸H. Shiba, *J. Phys. Soc. Jpn.* **55**, 2765 (1986).

⁹S. Sorella, E. Tosatti, S. Baroni, R. Car, and M. Parrinello, in *Towards the Theoretical Understanding of High-Temperature Superconductors*, Proceedings of the Adriatic Research Conference and Workshop, Trieste, Italy, edited by S. Lundquist *et al.* (World Scientific, Singapore, 1988), Vol. 14.

¹⁰R. Blankenbecler, D. J. Scalapino, and R. L. Sugar, *Phys. Rev. D* **24**, 2278 (1981).

¹¹P. W. Anderson, *Science* **235**, 1196 (1987).

¹²T. K. Lee and S. Feng, *Phys. Rev. B* **38**, 11809 (1988), C. Gros, *ibid.* **38**, 931 (1988).

¹³J. M. Luttinger, *Phys. Rev.* **119**, 1153 (1960).